Reversible Control over Molecular Recognition in Surface-Bound Photoswitchable Hydrogen-Bonding Receptors: Towards Read-Write-Erase Molecular Printboards

ARTICLE *in* CHEMISTRY · SEPTEMBER 2013

Impact Factor: 5.73 · DOI: 10.1002/chem.201301613 · Source: PubMed

8 AUTHORS, INCLUDING:

Galina Dubacheva
Ecole normale supérieure de Cachan
20 PUBLICATIONS **155** CITATIONS
SEE PROFILE

Cavagnat Dominique
Université Bordeaux 1
73 PUBLICATIONS **1,036** CITATIONS
SEE PROFILE

Bruno Fabre
Université de Rennes 1
127 PUBLICATIONS **1,724** CITATIONS
SEE PROFILE

James H R Tucker
University of Birmingham
82 PUBLICATIONS **1,310** CITATIONS
SEE PROFILE

CHEMISTRY
A EUROPEAN JOURNAL

ChemPubSoc
Europe

DOI: 10.1002/chem.201301613

Reversible Control over Molecular Recognition in Surface-Bound Photoswitchable Hydrogen-Bonding Receptors: Towards Read–Write–Erase Molecular Printboards

Chih-Kai Liang,[a] Galina V. Dubacheva,[a] Thierry Buffeteau,[a] Dominique Cavagnat,[a] Philippe Hapiot,[b] Bruno Fabre,[b] James H. R. Tucker,[c] and Dario M. Bassani*[a]

Abstract: The synthesis of an anthracene-bearing photoactive barbituric acid receptor and its subsequent grafting onto azide-terminated alkanethiol/Au self-assembled monolayers by using an Cu^{I}-catalyzed azide–alkyne reaction is reported. Monolayer characterization using contact-angle measurements, electrochemistry, and spectroscopic ellipsometry indicate that the monolayer conversion is fast and complete. Irradiation of the receptor leads to photodimerization of the anthracenes, which induces the open-to-closed gating of the receptor by blocking access to the binding site. The process is thermally reversible, and polarization-modulated IR reflection–absorption spectroscopy indicates that photochemical closure and thermal opening of the surface-bound receptors occur in 70 and 100% conversion, respectively. Affinity of the open and closed surface-bound receptor was characterized by using force spectroscopy with a barbituric-acid-modified atomic force microscope tip.

Keywords: anthracene · click chemistry · dimerization · molecular recognition · receptors

Introduction

Fabrication of molecule-based sensors or electronic devices requires spatial control of the molecular constituents over multiple length scales, a key step in the design and construction of hierarchically organized molecular assemblies in three dimensions.[1] For specific applications, such as in lab-on-chip devices, it can be advantageous to retain control over the active surface patterning until the final fabrication stages. Beyond this, on-the-fly control over the surface active area of a sensor during device operation would allow modulation of its sensitivity over many orders of magnitude, or even modification of its selectivity towards specific analytes. Several approaches have thus been pursued to develop so-called molecular printboards in which surface recognition is triggered with spatial resolution as a form of lithography.[2] A robust system based on the reversible formation of inclusion complexes between cavitands and adamantyls has been developed by Reinhoudt's group.[3] This allows supramolecular postmodification as a versatile alternative to microcontact printing approaches[4] for spatial control of surface functionality. In a different approach, developed by Matile's group, supramolecular interactions have been used to guide formation of covalent bonds between an initiator grafted onto a surface and a polymerizable unit in solution.[5] Along similar lines, we have explored the use of reversible covalent chemistry to fabricate hierarchical assemblies on surfaces.[6] All these methodologies are valuable and some have been implemented in the construction of functional devices for sensing[7] or solar energy conversion,[8] for example.

The grafting of molecular receptors with a binding constant that can be reversibly controlled by external means such as light would be particularly interesting for molecular printboards that possess read–write–erase capabilities. The potential of this approach was elegantly demonstrated by Mattay and co-workers by using a covalently grafted calixarene receptor appended with anthracene units, the dimerization of which was shown to gate the binding properties of the surface-bound receptor at the single-molecule level.[10] Like previous systems, the binding process relies on the formation of an inclusion complex driven by hydrophobic interactions. Selective interaction, such as that provided by a combination of hydrogen bonds, would offer the possibility of targeting specific architectures through a hierarchical

[a] Dr. C.-K. Liang, Dr. G. V. Dubacheva, Dr. T. Buffeteau, Dr. D. Cavagnat, Dr. D. M. Bassani
Institut des Sciences Moléculaires CNRS UMR5255
Univ. Bordeaux 1, 351, Cours de la Libération
33400 Talence (France)
Fax: (+33) 5-4000-6158
E-mail: d.bassani@ism.u-bordeaux1.fr

[b] Dr. P. Hapiot, Dr. B. Fabre
Institut des Sciences Chimiques de Rennes
Matière Condensée et Systèmes Electroactifs (MaCSE)
CNRS, UMR 6226, Université de Rennes 1
Campus de Beaulieu, Bat 10C, 35042 Rennes (France)

[c] Prof. J. H. R. Tucker
School of Chemistry
University of Birmingham
Edgbaston, Birmingham, B15 2TT (UK)

Supporting information for this article is available on the WWW under http://dx.doi.org/10.1002/chem.201301613.

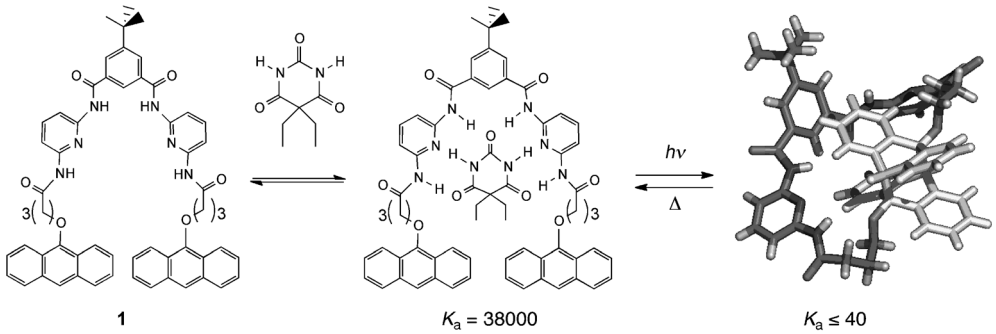

Figure 1. Receptor **1** uses anthracene photodimerization to control binding towards barbituric acid derivatives. The crystal structure of the intramolecular photodimer (right) indicates that access to the binding cleft is hindered upon dimerization.[9]

self-assembly approach. However, this has not been combined with photoactive gating to manufacture molecular printboards. Our previous work on photoactive receptors[6b,11] led us to develop a bis-anthracenyl receptor with a binding affinity towards barbituric acid that could be reversibly modulated from $K_a = 4 \times 10^4$ to $\leq 40\,\text{M}^{-1}$ (Figure 1).[9,12] We now report our investigation of the use of such systems to prepare photoactive substrates with an affinity towards barbituric acid that can be reversibly modulated and their application towards read–write–erase molecular printboards.

Molecular recognition of barbituric acid derivatives by **1** relies on the formation of multiple hydrogen-bonding interactions as previously developed by Hamilton and co-workers.[13] These receptors were later shown by Motesharei and Myles[14] to retain their affinity towards barbiturates once bound to gold substrates. Herein, we report the grafting of photoactive barbiturate receptors analogous to **1** onto gold substrates by using either a one-step thiol-on-gold procedure or through the postmodification of an azide-terminated self-assembled monolayer (SAM; Figure 2). Multiple techniques, such as atomic force microscopy (AFM), ellipsometry, polarization modulation IR reflection–absorption spectroscopy (PM-IRRAS), and surface wetting, were employed to characterize the transformation of the surface-bound receptor and its effect on the binding properties.

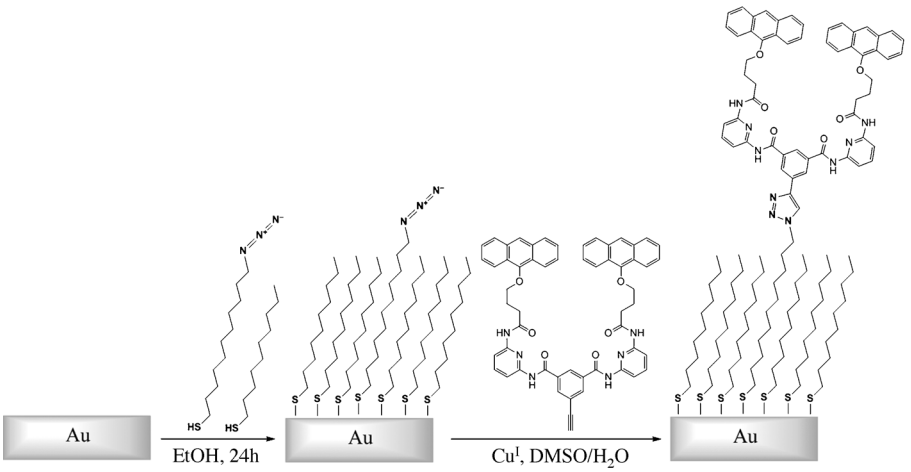

Figure 2. Two-step functionalization of gold surfaces: i) immobilization of azide-terminated thiols, and ii) immobilization of the photoactive barbiturate receptors through a Cu^I-catalyzed azide–alkyne click reaction (CuAAC reaction).

Results

The barbiturate receptors modified with various functionalities in the C-5 position of the central phenyl ring were obtained from a common iodine-substituted intermediate (**2**) prepared from 5-iodophthalic acid analogously to previously reported anthracene-appended receptors (Scheme 1). Sonogashira coupling was then used to introduce terminal functional groups suitable for direct or indirect immobilization onto various substrates. Full experimental details of the syntheses can be found in the Supporting Information.

We initially tested the one-step immobilization of thioacetate derivative (**3**) onto Au substrates by using different conditions of in situ deprotection of the thioacetate group.[15,16] Alkanethiol SAM was prepared by using the corresponding thioacetate and thiol derivatives and compared in terms of film thickness, homogeneity, and surface coverage. Spectroscopic ellipsometry was used to measure the film thickness (see Table S1 in the Supporting Information). However, imaging ellipsometry revealed the frequent presence of aggregates, and electrochemistry was therefore used to examine the interfacial capacitance before and after surface modification (Table S2 in the Supporting Information). The most homogeneous monolayers were obtained for samples prepared by using only *n*-alkanethiol derivatives.

In view of the difficulty of obtaining densely packed homogeneous monolayers that incorporate the desired receptor

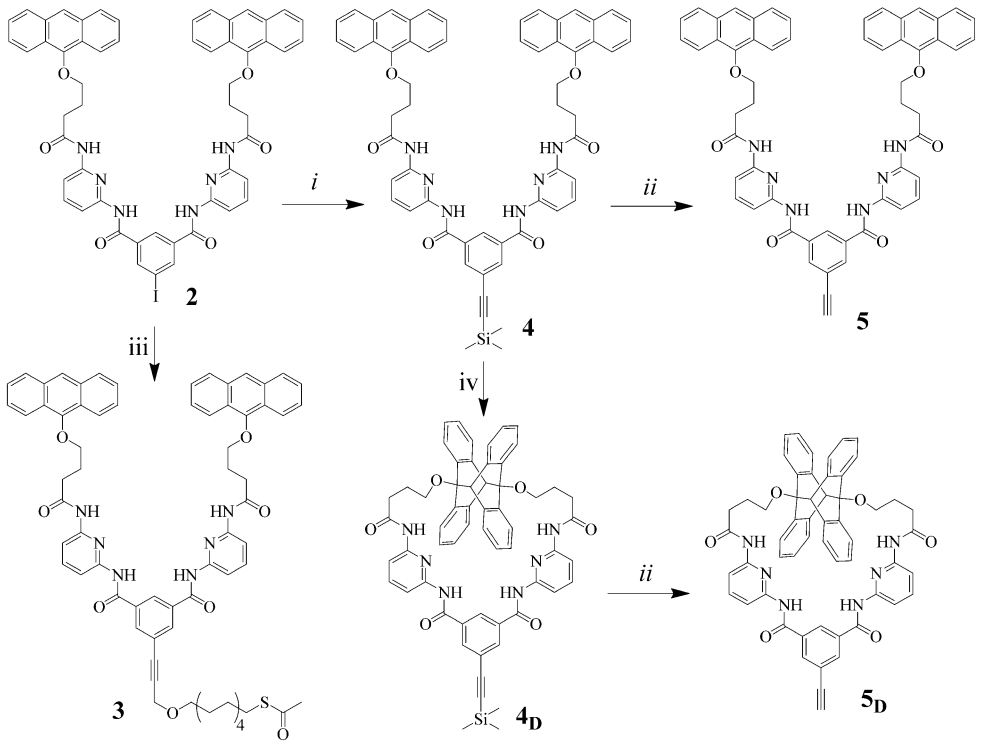

Scheme 1. Synthesis of anthracene-appended receptors. i) ethynyl(trimethyl)silane, $[Pd(PPh_3)_2Cl_2]$, CuI, PPh_3, *N*,*N*-diisopropylethylamine (DIEA), THF, RT; ii) LiOH, THF/H_2O, RT; iii) compound **6**, $[Pd(PPh_3)_2Cl_2]$, CuI, PPh_3, DIEA, THF, RT; iv) *hν*, CH_2Cl_2.

by using the direct approach, we turned to a two-step immobilization procedure that initially consisted of coadsorption of unfunctionalized and azide-terminated thiols to form a mixed monolayer (binary SAM), followed by a Cu^I-catalyzed azide–alkyne cycloaddition (CuAAC reaction) between the azide-terminated SAM and **5** (Figure 2).[17–19] Coupling of the azide groups in the binary SAM and **5** was carried out in water/DMSO by using Cu^I and tris[(1-benzyl-1*H*-1,2,3-triazol-4-yl)methyl]amine (TBTA) as catalyst (see the Supporting Information for experimental details) and followed by using spectroscopic ellipsometry to measure the film thickness. Prior to measurements, the surfaces were washed copiously with DMSO and water to remove all physisorbed species. Figure 3 shows the thickness of the receptor layer as a function of the $N_3C_{12}H_{24}SH$ mole fraction in the solution used to prepare the binary SAM. Low nonspecific binding of the receptor and the regular increase of the film thickness with increasing $N_3C_{12}H_{24}SH$ mole fraction indicates that the CuAAC reaction occurs efficiently and selectively. Increasing the reaction time from 3 to 5 h did not affect the measured receptor thickness. This attests to the fast kinetics of the covalent immobilization as previously reported for the immobilization of other molecules such as ferrocene and β-cyclodextrin using this approach.[18–20] The interfacial capacitance of the samples indicates that the substrates are covered with a compact monolayer, and the only features observed by AFM are those of the gold clusters (see Figure S1 in the Supporting Information).

The reaction of the terminal azide group can be expected to lead to a variation in the surface hydrophobicity, which can be followed using contact-angle goniometry after each step of the surface modification. Examples of images that show water droplets in contact with various substrates are

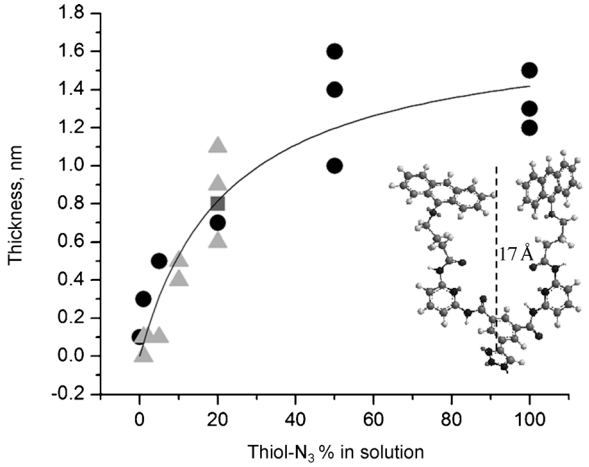

Figure 3. Thickness of the gold-bound receptor layer measured using spectroscopic ellipsometry after the CuAAC reaction plotted as a function of the $N_3C_{12}H_{24}SH$ molar fraction in solution. Reaction time: 3 h (black circles), 4 h (gray triangles), 5 h (gray squares). The solid line is a guide for the eyes. Inset: 3D molecular structure of the receptor attached to a surface by means of a CuAAC reaction. Molecular height was estimated for the most extended conformation in the direction perpendicular to the surface plane.

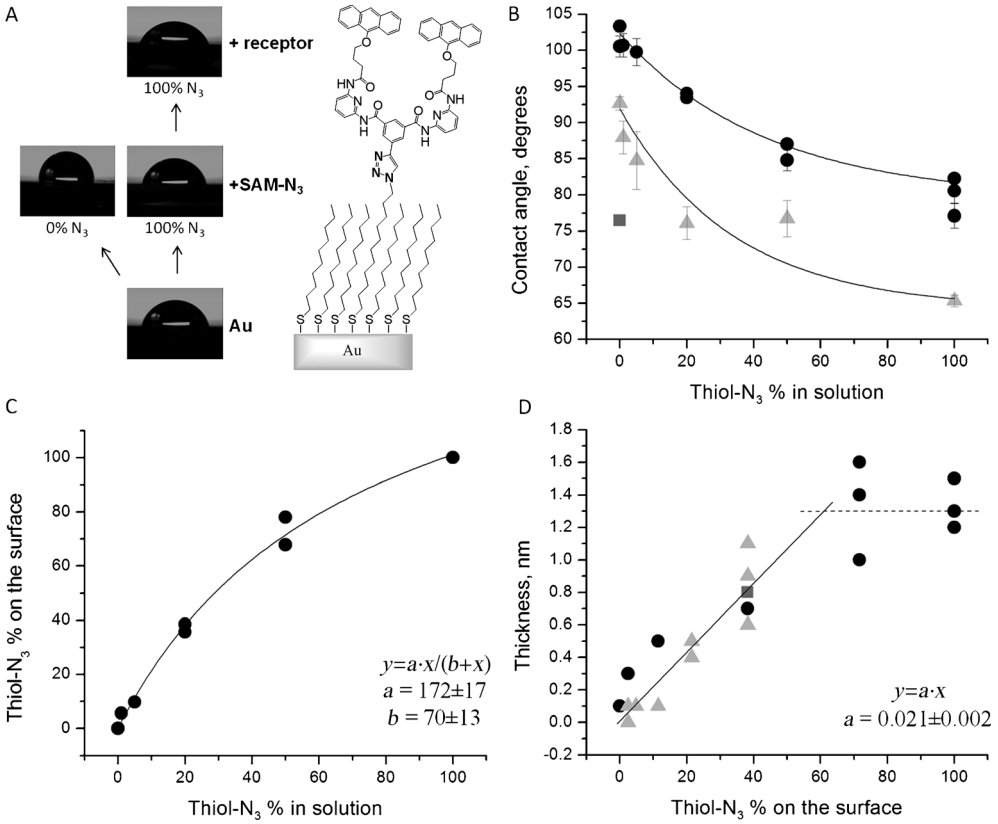

Figure 4. Contact-angle measurements: A) Examples of images showing a water droplet on a surface at different modification stages (left) together with the schematic representation of the molecular organization of the film (right). B) Contact angles measured on SAM-coated (black circles) and photoactive barbiturate receptor-modified (gray triangles) surfaces as a function of the $N_3C_{12}H_{24}SH$ mole fraction in the solution used to prepare binary SAMs. Bare gold surface is also characterized (gray squares). Solid lines are exponential fits to the points. C) The $N_3C_{12}H_{24}SH$ mole fraction on the surface as a function of the $N_3C_{12}H_{24}SH$ mole fraction in the solution used to prepare binary SAM. Solid lines are a guide for the eyes. D) Thickness of the photoactive barbiturate receptor layer (open configuration) measured by ellipsometry after CuAAC reaction plotted as a function of the $N_3C_{12}H_{24}SH$ molar fraction on the surface. Reaction time: 3 h (black circles), 4 h (gray triangles), 5 h (gray squares). The solid line is the linear best fit for $x<40\,\%$. The dashed line is the average thickness for $x>70\,\%$.

presented in Figure 4A. Figure 4B shows the contact angles plotted as a function of the $N_3C_{12}H_{24}SH$ mole fraction in the solution used to prepare the binary SAMs. One can see that gold surfaces that initially exhibit contact angles of 76° (Figure 4B, squares) became more hydrophobic after the formation of the SAM (Figure 4B, circles). Monolayers made from $C_{10}H_{21}SH$ alone exhibited contact angles of $(102\pm2)°$. However, fully azide-covered surfaces made from $N_3C_{12}H_{24}SH$ exhibited contact angles of $(80\pm3)°$. In view of control experiments on surface binding, modified substrates in which the terminal azide groups were reacted with **5D** were also prepared (see the Supporting Information).

The results are in good agreement with those obtained by Collman and co-workers for similar binary systems that involve methyl- ($\approx$110°) and azide- (77°) terminated thiols.[20] As expected, mixed monolayers exhibited contact angles that are intermediate between those of the pure monolayers of each single component. The surface became more hydrophilic after functionalization with **5** (Figure 4B, triangles). This can be explained by the interaction between water molecules and the hydrogen-bonding sites of the receptors. Remarkably, the evolution of the contact angles measured after immobilization of the receptor follows the same trend as that obtained for the azide surface concentration. It was shown for binary SAMs that the relation between the alkanethiol mole fraction in the solution and on the surface after SAM formation can be characterized by using contact-angle goniometry. Thus, the percentage of $N_3C_{12}H_{24}SH$ on a gold surface after the formation of binary mixed SAM was determined by using Cassie's law [Eq. (1)]:[21]

$$\cos\theta = f_1\cos\theta_1 + f_2\cos\theta_2 \quad (1)$$

in which θ, θ_1, and θ_2 are the contact angles on the mixed SAM and the two single-component SAM, respectively, and f_1 and f_2 are the mole fractions of each component present in the mixed SAM.[19,22] Figure 4C shows the percentage of $N_3C_{12}H_{24}SH$ on the gold surface (obtained by using Cassie's law) as a function of the molar fraction of $N_3C_{12}H_{24}SH$ in the solution used to prepare the mixed SAM. Since the relation between the $N_3C_{12}H_{24}SH$ mole fraction in the solution used to prepare the binary SAM and the $N_3C_{12}H_{24}SH$ mole fraction on a gold surface after SAM formation is known, one can plot the thickness of the receptor layer measured by

ellipsometry (Figure 3) as a function of the $N_3C_{12}H_{24}SH$ surface mole fraction. The resulting plot (Figure 4D) shows a linear increase of the receptor amount with the $N_3C_{12}H_{24}SH$ mole fraction until a saturation regime is achieved. It should be noted that the increase in height is solely due to the cycloaddition of **5** onto the binary monolayer, and thus reflects the surface density of **5** as ellipsometry will return an average thickness value. The measurement is, however, independent of the tilt angle of the alkanethiols with respect to the surface because this is not expected to vary upon reaction of the terminal azide groups with **5**. As mentioned earlier, for high azide coverage there is a steric limit to the amount of the receptor that can be immobilized. Therefore, it is not surprising that the approximately linear relationship between the receptor layer thickness and azide surface density becomes nonlinear with greater azide coverage. Importantly, the linear increase at low azide coverage shows that the CuAAC modification is quantitative, and that the amount of receptor on the substrate can be tuned by choosing the appropriate $N_3C_{12}H_{24}SH/C_{10}H_{21}SH$ ratio in solution during SAM formation.

Although FTIR spectroscopy has been used to follow anthracene photodimerization on surfaces,[10b] PM-IRRAS presents significant advantages in terms of sensitivity and selectivity towards surface-bound species.[23] Herein, it was used to obtain information on the density and conformation of the functional groups in the SAMs that comprise receptor **5** and $\mathbf{5_D}$. The p- and s-polarized germanium attenuated total reflection (Ge-ATR) spectra were first recorded to check whether a preferential orientation of the open and closed receptor molecules occurs after deposition onto the crystal, thus leading to anisotropic optical constants. As shown in Figure S2 of the Supporting Information, the p-polarized ATR spectra of the open and closed receptors have twice the intensity of the s-polarized ones over the entire spectral range, which is in agreement with an isotropic arrangement of the molecules at the crystal surface. As a consequence, the optical constants determined from the polarized ATR spectra are similar in the plane (xy) and out of the plane (z) of the layers. The variation in the isotropic refractive indexes $n(\tilde{\nu})$ and extinction coefficients $k(\tilde{\nu})$ are reported in Figure S3 of the Supporting Information in the 4000–600 cm^{-1} spectral range for the two molecules.

The isotropic extinction coefficients $k(\tilde{\nu})$ of the open and closed receptors are reported in Figure 5 in the 1800–1000 cm^{-1} spectral range. The $k(\tilde{\nu})$ spectra can be used to assign the major IR bands of the receptor. This assignment has been performed on the basis of data in the literature[24] and from calculations of the optimized geometries, vibrational frequencies, and IR intensities of the molecules using Gaussian 09 package (see the Supporting Information). These calculations have been performed at the DFT level using the B3PW91 functional and the 6-31G* basis set. The wavenumbers, assignment, and origin of the different infrared bands are given in Table 1. The three bands at 1415, 1390, and 1340 cm^{-1} have been chosen to follow the open and closed forms of the receptor because they are easily discernible from the other bands of the receptor. The bands at 1415 and 1340 cm^{-1} can be assigned to the νC=C stretching vibration of the central ring of anthracene coupled with the δC=C-H bending vibration and the νC−O stretching vibration, respectively. Finally, the band at 1390 cm^{-1} can be assigned to the ωCH_2 wagging vibrations of the three methylene units linked to the anthracene and to the photodimer. This band exhibits a medium intensity for the closed receptor, whereas its intensity is very low for the open receptor.

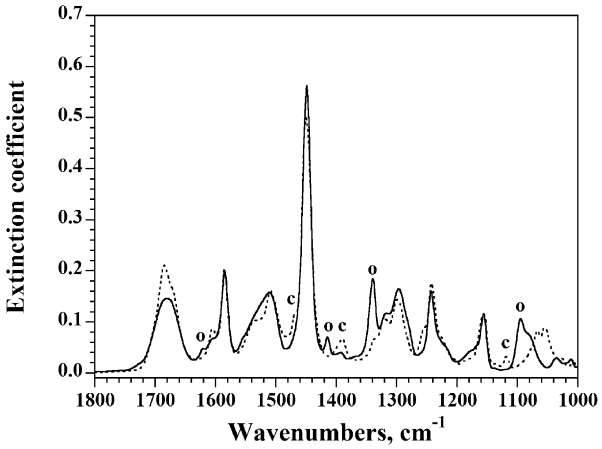

Figure 5. Isotropic extinction coefficients $k(\tilde{\nu})$ of the open **5** (solid line) and closed $\mathbf{5_D}$ (dashed line) receptors determined from ATR IR measurements. The bands assigned to the open and closed (photodimer) receptor are labeled o and c, respectively.

Table 1. Energy, assignment, and origin of the major bands in **5** and $\mathbf{5_D}$.

Position [cm^{-1}]	Assignment	Origin
1680	νC=O	amide
1621	νC=C + δC=C−H (external ring)	anthracene
1605, 1585	νC=C	pyridine
1511	δNH	amide
1469	νC=C + δC=C−H (external ring)	photodimer
1449	νC=C	pyridine
1415	νC=C (central ring) + δC=C−H	anthracene
1390	ωCH_2 ($3\,CH_2$ linked to photodimer)	photodimer
1340	νC=C (central ring) + νC−O	anthracene
1296	νN=C + νC=C	pyridine
1242	νN=C + νC=C	pyridine
1155	δC=C−H	pyridine
1118	δC−H + νC−O	photodimer
1095	δC=C−H	anthracene

The PM-IRRAS spectra of the azide- and **5**-terminated SAMs are shown in Figure S4 of the Supporting Information, whereas those of monolayers that contain open, closed, and mixed (prepared from 1:1 solutions of **5** and $\mathbf{5_D}$) receptors are reported in Figure S5 of the Supporting Information. These spectra exhibit bands at 2920 and 2850 cm^{-1}, which are assigned to the asymmetric ($\nu_a CH_2$) and symmetric ($\nu_s CH_2$) stretching vibrations of the methylene groups; at 2105 cm^{-1}, they are assigned to asymmetric stretching vibra-

tion of the azide groups; and at wavenumbers lower than 1800 cm^{-1}, they are assigned to the vibrations of the receptor (see above). First of all, it is worth noting that the PM-IRRAS spectra were obtained with a very good signal-to-noise ratio, thereby allowing observation of the chemical modification of the receptor. Indeed, the 1440–1260 cm^{-1} region (Figure 6) clearly reveals the presence of monosubsti-

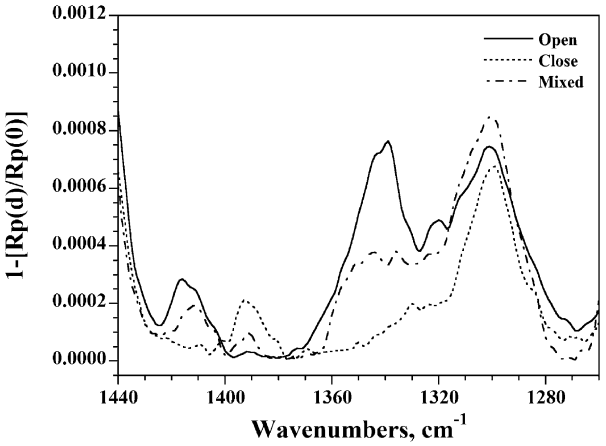

Figure 6. Portion of the PM-IRRAS spectra of SAMs containing open **5** (solid line), closed $\mathbf{5_D}$ (dotted line), and mixed $\mathbf{5/5_D}$ (dotted/dashed line) receptors. See Figure S5 in the Supporting Information for the full spectra.

tuted anthracene (bands at 1415 and 1340 cm^{-1}) for the open form of the receptor and the presence of photodimer (band at 1390 cm^{-1} accompanied by the disappearance of the bands at 1415 and 1340 cm^{-1}) for the closed form of the receptor. The PM-IRRAS spectrum of the monolayer that contains a 1:1 mixture of open and closed receptors exhibits bands at 1415, 1390, and 1340 cm^{-1} with intermediate intensities. Furthermore, the wavenumbers observed for the ν_aCH_2 (2920 cm^{-1}) and ν_sCH_2 (2850 cm^{-1}) vibrations of the methylene groups are indicative of an ordered arrangement of the alkyl chains with a preferential all-*trans* conformation. Indeed, these two modes are reported typically to be in the range 2915–2918 and 2846–2850 cm^{-1} for all-*trans* extended chains[25] and at approximately 2928 and approximately 2856 cm^{-1} for liquidlike disordered chains.[26] Finally, the presence of a significant $\nu_aN{=}N{=}N$ band at 2105 cm^{-1} reveals that only a part of the SAM-$C_{12}H_{24}N_3$ reacted with **5** or $\mathbf{5_D}$.

The proportion of azide groups which have reacted with the receptor can be easily determined by comparing the PM-IRRAS spectra of a SAM-$C_{12}H_{24}N_3$ before and after coupling with **5**, as shown in Figure S4 of the Supporting Information. The decrease in the intensity of the $\nu_aN{=}N{=}N$ band at 2105 cm^{-1} is directly associated with the conversion of the azide groups. The percentage of azide conversion was calculated to be $(41\pm2)\%$ over four different samples of open and closed receptors (**5** and $\mathbf{5_D}$; see Table S3 in the Supporting Information for more information).

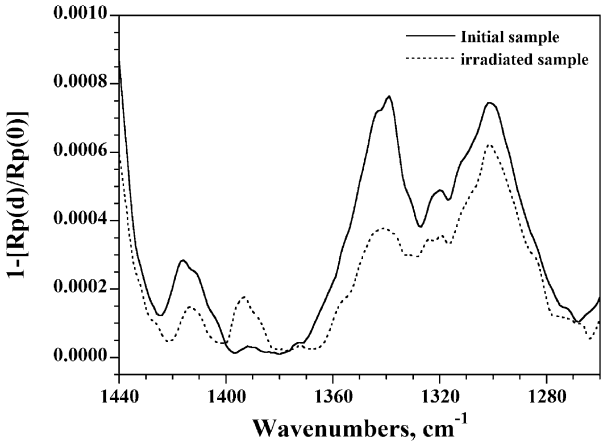

Figure 7. Portion of the PM-IRRAS spectra of SAM containing receptor **5** before (solid line) and after (dashed line) irradiation. See Figure S6 in the Supporting Information for the full spectra.

The open→closed conversion of the receptor by irradiation was followed using PM-IRRAS. In Figure 7 (see Figure S6 in the Supporting Information for the full spectra), the PM-IRRAS spectrum of the monolayer that contains the receptor in the open form is compared to that of the same sample following 20 min of irradiation at 365 nm in a degassed liquid environment (dichloromethane). Figure S6 in the Supporting Information shows an overall decrease in PM-IRRAS intensities of about 20% for the irradiated sample. Since all the bands are affected, we can affirm that a small amount of molecules were lost during the conversion procedure. The zoom in the 1440–1260 cm^{-1} region (Figure 7) shows that the bands at 1415 and 1340 cm^{-1}, which are related to monosubstituted anthracene, decrease, whereas the band at 1390 cm^{-1}, which is related to the photodimer, appears. This result clearly indicates that the open→closed conversion of the surface-bound receptor occurs during irradiation. By using the intensity of the 1340 cm^{-1} band, we can estimate a conversion of about 70% of the grafted anthracene chromophores. Further irradiation did not result in an increased proportion of photodimerized product.

The closed→open conversion of the photoirradiated receptor was achieved by briefly heating the sample at 80°C and was also followed by PM-IRRAS. The PM-IRRAS spectrum of irradiated **5**-containing monolayer is compared in Figure 8 (see Figure S7 in the Supporting Information for full spectra) to that of the same sample after heating at 80°C (20 min). As shown in Figure S7 of the Supporting Information, the intensities of the major bands remain unchanged, thus indicating that no degradation of the SAM occurs during heating. However, a very small disorder of the alkyl chains is observed for the heated sample, as seen in Figure S8 of the Supporting Information, through an increase in the width and the intensity of the ν_aCH_2 and ν_sCH_2 bands. The widening of these bands is attributed to the presence of alkyl chains with *gauche* defects, thereby giving rise to absorptions at higher wavenumbers (≈2928 and

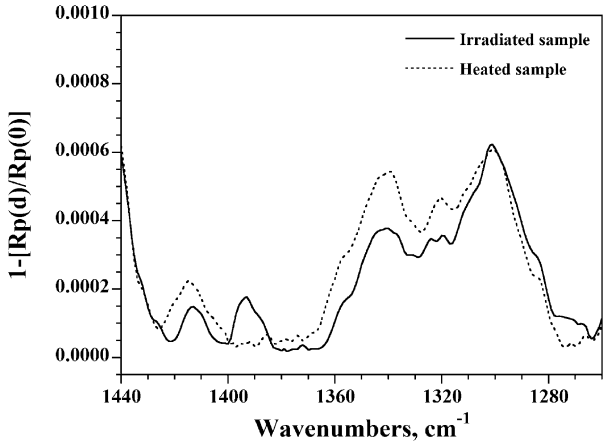

Figure 8. Portion of the PM-IRRAS spectra of irradiated SAM containing receptor **5** before (solid line) and after (dashed line) heating at 80 °C. See Figure S7 in the Supporting Information for the full spectra.

$\approx$2856 cm^{-1}), whereas the increase in the intensities is due to the fact that the projection of the transition moments of the methylene modes is most favorable when the chains are not perpendicular to the substrate (surface selection rule of the PM-IRRAS). Nevertheless, the disorder of the alkyl chains is very low with respect to those published in the literature for heated Langmuir–Blodgett monolayers.[27] Finally, the zoom in the 1440–1260 cm^{-1} region (Figure 8) shows that the bands at 1415 and 1340 cm^{-1} increase, whereas the band at 1390 cm^{-1} vanishes. This result clearly indicates that the closed→open conversion of the receptor occurs quantitatively.

The emission spectrum of **5** in solution and of a monolayer that contains the open receptor are shown in Figure 9. The maximum emission of the fluorescence from the anthracene chromophore in the monolayer is located at 440 nm,

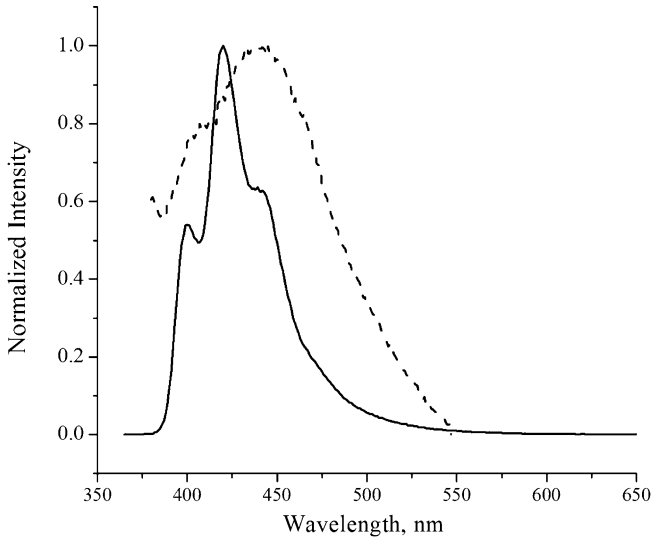

Figure 9. Comparison of the fluorescence emission spectra (λ_{ex} = 370 nm) between **5** in solution (CH_2Cl_2, solid line) and immobilized on a gold surface (dashed line).

which corresponds to a 20 nm bathochromic shift relative to the emission in solution. The emission is also somewhat broader, which suggests the occurrence of enhanced excimer emission.[12] Little or no luminescence was collected from substrates functionalized with the closed receptor $\mathbf{5_D}$.

To study the molecular recognition properties of the immobilized barbiturate receptors, we performed force spectroscopy measurements using surfaces modified with receptors (open or closed).[28] The AFM cantilevers were functionalized with a thiol-tethered barbituric acid (compound **6**; Figure 10A).[8c,29] The representative force/distance curves obtained in these measurements are also shown. The force profiles represent the interaction forces upon approach (Figure 10A, red trace) and retraction (Figure 10A, blue trace) as a function of the separation distance between the surface and the tip. When approaching the sample surface with the AFM probe, no interaction forces were detected. Upon contact, the tip was pressed against the surface up to a set maximum loading force of 2.5 nN. After reaching the maximal force, the two surfaces remained in contact for a time interval of 5 s, after which the direction of the piezo movement was reversed, and the AFM probe was retracted from the surface. The interaction between the immobilized receptor and barbituric acid attached to the AFM tip was probed during the retraction part of the force profile. Figure 10A shows the most frequent force spectroscopy responses classified as "no event" and "single event."

Several sets of force spectroscopy experiments were performed on different monolayers with modified and unmodified tips. One set of measurements was done on surfaces modified with open or closed receptors using AFM tips modified with a barbiturate-appended thiol derivative (compound **6**;[8c,30] Figure 10). The force histogram that characterizes the interaction that occurs on the surface functionalized with the open receptor is shown in Figure 10B. About half of the retraction curves exhibited single binding events, which yielded a force histogram with an overall binding probability of 51 % and a dissociation single event force of 172 pN. One might notice an additional binding event at 350 pN, which corresponds to twice the force of the single event and is therefore assigned to the simultaneous breaking of two barbituric acid–receptor interactions. A comparison of the two force spectroscopy measurements performed on different open receptor-modified surfaces and by using different barbiturate-modified cantilevers shows the high reproducibility of the results: Both the overall binding probability and the most frequent dissociation single event force differ within an error of less than 10 % (Figure 10B). The force histogram that characterizes the binding to the surface modified with $\mathbf{5_D}$ is shown in Figure 10C. A single binding event with a force equal to 169 pN and a probability of 13 % was detected.

An additional set of measurements was done on the receptor-modified gold surfaces by using unmodified (bare) AFM tips as controls (Figure S8 in the Supporting Information). The probability force histograms that characterize the interactions between the unmodified AFM tip and the surfa-

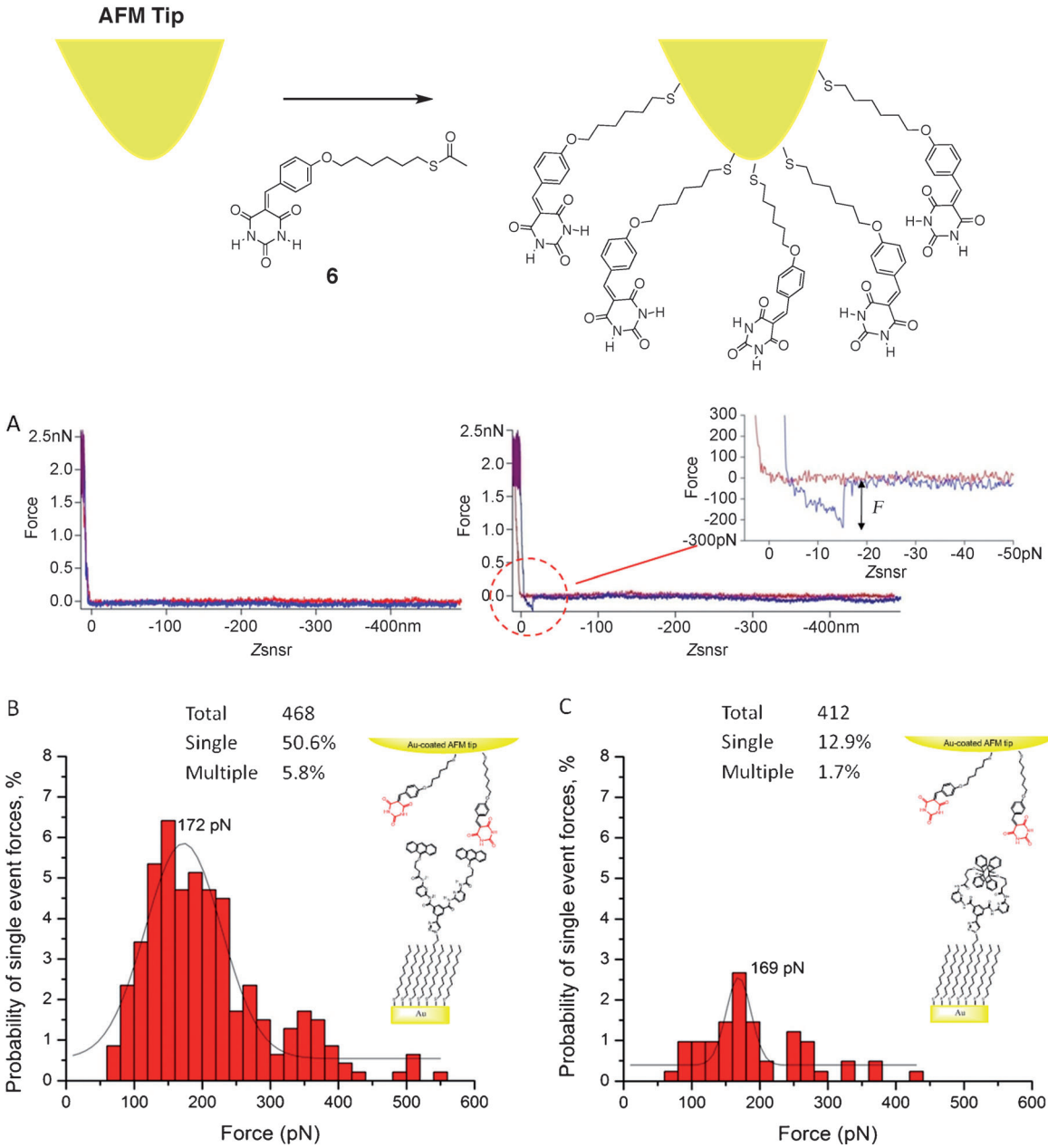

Figure 10. AFM force measurements using an AFM tip modified with **6**. A) Representative force/distance curves showing profiles classified as "no event" and "single event." B, C) Probability of single event forces plotted as a function of the interaction force measured by AFM using barbiturate-modified AFM tip and gold-surface-functionalized with the receptor in the open (B) or closed (C) configuration. Solid lines are the Guassian fits. The total amount of the analyzed events together with the percentage of single and multiple events are presented in each case.

ces functionalized with open or closed receptor did not exhibit any Gaussian distribution. Moreover, the overall binding probability was found to be less than 5%. This indicates that the recognition events registered when using the functionalized AFM tips are due to the specific interactions between the barbiturate receptor attached to the surface and the barbituric acid attached to the AFM tip.

To study the affinity modulation upon photoswitching of the surface-confined receptors, we measured the interaction forces at surfaces modified with the open receptor before and after photoirradiation at 350–390 nm. To increase the distance between the receptor functions at the surface, the $N_3C_{12}H_{24}SH/C_{10}H_{21}SH$ molar ratio in the solution used to prepare binary SAMs for these experiments was fixed at 0.01. After 15 min of irradiation, the probability of the most frequent single event force decreased from 7.8 to 6.5%. After additional 45 min of irradiation, it further decreased to 4.5%. The range of single event forces remained the same except for the peak at 350 pN, which disappeared after irradiation (see Figure S9 in the Supporting Information).

Discussion

The formation of compact monolayers that contain open or closed receptor-terminated alkanethiols directly from thioacetate-protected thiols did not prove sufficiently reliable. One can explain the poor molecular order of the SAMs thus obtained by the inefficient in situ cleavage of the thioacetate precursor, which resulted in their initial physisorption onto the surface in a way that might inhibit the formation of highly ordered and densely packed phases.[31] Therefore, the use of a two-step procedure for the immobilization of **5** and $\mathbf{5_D}$ based on the formation of an azide-terminated binary SAM followed by the covalent attachment of the receptor (Figure 2) by means of CuAAC was selected to avoid this problem.[17,18,32] The concomitant deposition of binary SAMs from thioalkane mixtures in solution was expected to lead to homogeneous dispersions.[33] The thickness of the receptor layer obtained using this procedure increased smoothly with increasing $N_3C_{12}H_{24}SH$ mole fraction until a saturation regime was achieved. This saturation can be explained by the steric bulk of the receptor molecules that prevents further conversion of the remaining azides at high surface densities.[18–20] The maximal increase in thickness obtained for the receptor layer (1.6 nm, without taking into account the thickness of the underlying SAM) is in good agreement with the length of the extended molecule estimated by molecular modeling (Figure 3). This suggests that the CuAAC reaction leads to the formation of densely packed receptor monolayers at high thiol–azide molar fractions.

Contact-angle measurements indicate that the $N_3C_{12}H_{24}SH$ mole fraction on the Au surface is higher than that in solution (Figure 4C). This result is in agreement with the study reported by Bain and Whitesides et al., which shows the preferential adsorption of alkanethiols that have longer chains ($N_3C_{12}H_{24}SH$ versus $C_{10}H_{21}SH$ in this case) from ethanol solutions on gold surfaces.[34] By using this data, it is possible to plot the thickness of the receptor layer measured by ellipsometry as a function of the azide mole fraction on the surface (Figure 4D). The resulting plot shows a linear increase of the receptor amount with the $N_3C_{12}H_{24}SH$ mole fraction until a saturation regime is achieved at approximately 50–60 % azide coverage. Beyond this value, the presence of additional azide functionalities does not lead to a greater proportion of open receptor being grafted onto the monolayer. As mentioned earlier, there is a steric limit to the amount of the receptor that can be immobilized at high azide coverage due to the molecular footprint of the receptor moiety, and it is therefore not surprising that the linear relationship between the receptor layer thickness and azide surface density levels off at higher surface azide coverage. More importantly, the linear increase at low azide surface concentrations shows that the CuAAC modification is quantitative and that the amount of photoactive barbiturate receptor on the substrate can be tuned by choosing the appropriate $N_3C_{12}H_{24}SH/C_{10}H_{21}SH$ ratio in solution during SAM formation.

PM-IRRAS provides information on the chemical composition of the SAMs prepared as well as the conformation of the alkyl chains and the orientation of the functional groups. From the residual azide absorption, a conversion of terminal azide groups following CuAAC reaction with **5** of approximately 40 % can be estimated. This is close to the value obtained from contact-angle measurements by using Cassie's law. Assuming a homogeneous dispersion of azide functional groups on the surface (with approximately 25 $Å^2$ chain packing density)[35] and a conversion of 40 %, we can deduce that the surface area occupied by **5** is approximately 60 $Å^2$.

Comparison of the vibrational spectra of the surface-bound open and closed receptors revealed differences in the 1440–1260 cm^{-1} region, in which vibrations attributed to the central anthracene ring are expected. The absorptions in this region are characteristic of the open or closed receptor and can be used to determine the relative proportions of closed and open receptors in a monolayer. Thus, it could be determined that 70 % of surface-bound open receptors underwent photodimerization upon exposure to 365 nm light for 20 min. The incomplete conversion to photodimerized (i.e., closed) receptor might arise from the high surface density of receptors used for the PM-IRRAS experiments, which might limit conformational mobility of the anthracenes and hence impede their photodimerization. We might also expect competition between intramolecular photodimerization and photodimerization of anthracenes belonging to adjacent receptor molecules. In the latter event, a pair of anthracenes would be left unreacted and, in the absence of a nearby anthracene moiety with which to dimerize, would remain photostable. Interestingly, the emission spectrum of the open receptor grafted onto the surface exhibits a significant bathochromic shift with respect to solution. Weak excimer emission has been previously detected in solution from such linked bis-anthracene receptors,[12,36] and it seems probable that their immobilization onto a surface enhances excimer formation. Thermal treatment of the samples afforded complete conversion to the open receptors, as expected for thermally labile anthracene [4+4] photodimers.[9–10,37]

The photoinduced gating of the binding ability of the surface-bound receptor towards barbiturates was probed by using force spectroscopy.[38] This technique allows the detection of the probability of binding events as a modified AFM tip is brought into contact and retracted from the substrate and has been previously applied to characterize gating of a bis-anthracene resorc[4]arene receptor.[10a] Control experiments on monolayers grafted with open and closed receptor clearly indicate that the former possesses a much greater probability of a specific interaction (attributed to host–guest binding) towards the modified tip. The smaller number of recognition events detected at the surface modified with the closed receptor (Figure 10C) results from nonspecific adhesion (also seen in control experiments with unmodified tips or thioalkane monolayers; see the Supporting Information) along with a trace amount of open receptor resulting from incomplete photodimerization and/or gradual reopening of the receptor molecules over time. The HPLC analysis of the

photodimerized receptor $\mathbf{5_D}$ showed approximately 2% residual **5** to be present.

The decrease in the probability of binding events upon irradiation of the open receptor substrates is assigned to the photodimerization of the anthracene moieties, as supported by the PM-IRRAS experiments, which leads to a diminished binding affinity of the receptor. However, unlike the resorc[4]arene system in which a tenfold reduction in binding probability is observed upon irradiation, the reduction in binding probability is only twofold. Despite a tenfold dilution of the surface concentration of the receptor relative to the control force spectroscopy experiments above,[39] a binding event at 370 pN can still be observed. This might indicate a preference for the receptor molecules to aggregate on the surface, which would diminish their photodimerization efficiency as observed in the PM-IRRAS experiments. Furthermore, a higher local concentration of receptors increases the likelihood that the functionalized AFM tip can make contact with at least one open receptor molecule.

Conclusion

The development of molecular printboards based on photoaddressable hydrogen-bonding receptors immobilized onto a substrate is attractive because it combines straightforward patterning with the possibility of high selectivity towards specific substrates, which is desirable for the construction of hierarchically organized assemblies on surfaces and the selective detection of selected analytes. However, the chemical complexity of these receptors might render the direct fabrication of homogeneous monolayers difficult, and we find that a two-step procedure that involves chemical postmodification of a compact well-defined monolayer to be more practical. The use of anthracene photodimerization to restrict the access of the guest to the binding site, although effective in solution, appears to be less efficient when the same hosts are immobilized onto a substrate. One evident difficulty is reconciling a high surface density of photoactive receptors while minimizing intermolecular photoreactions. In contrast, the thermal regeneration of the open receptor is efficient, and this bodes well for their use in future read–write–erase molecular printboards. More generally, as recently discussed by Matile and co-workers,[40] the fidelity of the transcription process that conveys information from the surface-bound monolayer to the supramolecularly bound architectures must be high to reduce the accumulation of errors in the ensuing assemblies. Further work on the applications of this system towards photolithography and the construction of hierarchical self-assembled architectures on surfaces is ongoing.[41]

Experimental Section

SAM formation: SAM-coated gold surfaces were prepared by dipping a clean gold substrate into a solution of the desired thiol or a mixture of thiols in absolute ethanol at room temperature. After SAM formation, the gold surfaces were rinsed, dried, and immersed at room temperature into a water/DMSO (1:2) solution that contained 0.5 mM receptor alkyne (in the open or closed state), 0.5 mM $CuSO_4$, 0.5 mM tris[(1-benzyl-1*H*-1,2,3-triazol-4-yl)methyl]amine (TBTA), and 2.8 mM sodium ascorbate for 3–5 h. Exposure to light was kept to a minimum. After reaction, the monolayers were rinsed with water and DMSO to ensure that all physisorbed molecules were washed off.

Photodimerization of the receptors

In solution: A solution filter (lead nitrate/potassium bromide; $Pb(NO_3)_2$ (7 g L^{-1})/KBr (540 g L^{-1})) was used to cut off the UV light below 350 nm. The light source was a Hanovia 450 W HgXe lamp. During the irradiation, a continuous bubbling of argon or nitrogen was necessary to avoid photooxidation. The reaction was monitored by UV-absorption spectroscopy with the absorption band at 370 nm.

On the surface: The surfaces functionalized with open receptors were dipped in toluene and photoirradiated at 350–390 nm. The irradiation was carried out under argon to prevent photooxidation. The irradiation time was varied from 15 to 60 min.

PM-IRRAS measurements: PM-IRRAS spectra were recorded using a ThermoNicolet Nexus 670 FTIR spectrometer at a resolution of 4 cm^{-1} by co-adding several blocks of 1500 scans (30 min acquisition time). Generally, eight blocks (4 h acquisition time) were necessary to obtain PM-IRRAS spectra of SAMs with good signal-to-noise ratios. Experiments were performed at an incidence angle of 75° by using an external home-made goniometer reflection attachment and adding a ZnSe photoelastic modulator (PEM, Hinds Instruments, type III) after the polarizer.[23a,c] PM-IRRAS spectra are presented in terms of the IRRAS unit by using a calibration procedure.[23b,c] See the Supporting Information for details.

AFM measurements: AFM measurements were acquired using an MFP-3D atomic force microscope (Asylum Research) by using gold-coated Si cantilevers (Cont-GB from Budget Sensors with a force constant of 0.2 N m^{-1} and resonance frequency of 13 kHz). These were modified with a thiol-appended barbiturate by dipping the tip into a solution of **6**[8c] in THF overnight (1 mM in Et_3N (15%)/THF solution; see the Supporting Information for details). All force spectroscopy measurements were performed in 1,2-dichlorobenzene at room temperature. Force/distance traces were recorded at approach and retraction velocities of 250 nm s^{-1} with contact time of 5 s. The maximum loading force against the substrate after the contact was below 2.5 nN. Force/distance curves were collected from several different positions on the substrate, and about 50 force curves were measured at each position. See the Supporting Information for details.

Acknowledgements

Financial support from the CNRS and the Agence Nationale de la Recherche (ANR-08-BLAN-0161, project HI-LIGHT) is gratefully acknowledged.

[1] a) R. Bhosale, J. Misek, N. Sakai, S. Matile, *Chem. Soc. Rev.* **2010**, *39*, 138; b) G. V. Dubacheva, C. K. Liang, D. M. Bassani, *Coord. Chem. Rev.* **2012**, *256*, 2628; c) V. Palermo, P. Samori, *Angew. Chem.* **2007**, *119*, 4510; *Angew. Chem. Int. Ed.* **2007**, *46*, 4428.

[2] a) M. J. W. Ludden, D. N. Reinhoudt, J. Huskens, *Chem. Soc. Rev.* **2006**, *35*, 1122; b) P. Maury, M. Peter, O. Crespo-Biel, X. Y. Ling, D. N. Reinhoudt, J. Huskens, *Nanotechnology* **2007**, *18*, 044007.

[3] a) J. Huskens, M. A. Deij, D. N. Reinhoudt, *Angew. Chem.* **2002**, *114*, 4647; *Angew. Chem. Int. Ed.* **2002**, *41*, 4467; b) F. Corbellini, A. Mulder, A. Sartori, M. J. W. Ludden, A. Casnati, R. Ungaro, J. Huskens, M. Crego-Calama, D. N. Reinhoudt, *J. Am. Chem. Soc.* **2004**, *126*, 17050; c) H. Xu, X. Y. Ling, J. van Bennekom, X. Duan, M. J. W. Ludden, D. N. Reinhoudt, M. Wessling, R. G. H. Lammertink, J. Huskens, *J. Am. Chem. Soc.* **2009**, *131*, 797.

[4] a) N. L. Jeon, I. S. Choi, G. M. Whitesides, N. Y. Kim, P. E. Laibinis, Y. Harada, K. R. Finnie, G. S. Girolami, R. G. Nuzzo, *Appl. Phys. Lett.* **1999**, *75*, 4201; b) G. M. Whitesides, E. Ostuni, S. Takayama, X. Jiang, D. E. Ingber, *Annu. Rev. Biomed. Eng.* **2001**, *3*, 335; c) J. Lahiri, E. Ostuni, G. M. Whitesides, *Langmuir* **1999**, *15*, 2055.

[5] a) N. Sakai, M. Lista, O. Kel, S.-i. Sakurai, D. Emery, J. Mareda, E. Vauthey, S. Matile, *J. Am. Chem. Soc.* **2011**, *133*, 15224; b) P. Charbonnaz, N. Sakai, S. Matile, *Chem. Sci.* **2012**, *3*, 1492; c) M. Lista, E. Orentas, J. Areephong, P. Charbonnaz, A. Wilson, Y. Zhao, A. Bolag, G. Sforazzini, R. Turdean, H. Hayashi, Y. Domoto, A. Sobczuk, N. Sakai, S. Matile, *Org. Biomol. Chem.* **2013**, *11*, 1754.

[6] a) B. Fabre, D. M. Bassani, C. K. Liang, D. Ray, F. Hui, P. Hapiot, *J. Phys. Chem. C* **2011**, *115*, 14786; b) D. Ray, C. Belin, F. Hui, B. Fabre, P. Hapiot, D. M. Bassani, *Chem. Commun.* **2011**, *47*, 2547.

[7] a) M. J. W. Ludden, A. Mulder, R. Tampe, D. N. Reinhoudt, J. Huskens, *Angew. Chem.* **2007**, *119*, 4182; *Angew. Chem. Int. Ed.* **2007**, *46*, 4104; b) M. D. Yilmaz, S.-H. Hsu, D. N. Reinhoudt, A. H. Velders, J. Huskens, *Angew. Chem.* **2010**, *122*, 6074; *Angew. Chem. Int. Ed.* **2010**, *49*, 5938; *Angew. Chem.* **2010**, *122*, 6074.

[8] a) N. Sakai, S. Matile, *J. Am. Chem. Soc.* **2011**, *133*, 18542; b) G. Sforazzini, R. Turdean, N. Sakai, S. Matile, *Chem. Sci.* **2013**, *4*, 1847; c) C. H. Huang, N. D. McClenaghan, A. Kuhn, G. Bravic, D. M. Bassani, *Tetrahedron* **2006**, *62*, 2050.

[9] Y. Molard, D. M. Bassani, J.-P. Desvergne, P. N. Horton, M. B. Hursthouse, J. H. R. Tucker, *Angew. Chem.* **2005**, *117*, 1096; *Angew. Chem. Int. Ed.* **2005**, *44*, 1072.

[10] a) C. Schäfer, R. Eckel, R. Ros, J. Mattay, D. Anselmetti, *J. Am. Chem. Soc.* **2007**, *129*, 1488; b) M. Michelswirth, M. Rakers, C. Schafer, J. Mattay, M. Neumann, U. Heinzmann, *J. Phys. Chem. B* **2010**, *114*, 3482; c) V. Walhorn, C. Schafer, T. Schroder, J. Mattay, D. Anselmetti, *Nanoscale* **2011**, *3*, 4859.

[11] a) V. Darcos, K. Griffith, X. Sallenave, J. P. Desvergne, C. Guyard-Duhayon, B. Hasenknopf, D. M. Bassani, *Photochem. Photobiol. Sci.* **2003**, *2*, 1152; b) D. M. Bassani, X. Sallenave, V. Darcos, J. P. Desvergne, *Chem. Commun.* **2001**, 1446; c) Y. V. Pol, R. Suau, E. Perez-Inestrosa, D. M. Bassani, *Chem. Commun.* **2004**, 1270; d) C. H. Huang, D. M. Bassani, *Eur. J. Org. Chem.* **2005**, 4041.

[12] Y. Molard, D. M. Bassani, J.-P. Desvergne, N. Moran, J. H. R. Tucker, *J. Org. Chem.* **2006**, *71*, 8523.

[13] a) S. K. Chang, A. D. Hamilton, *J. Am. Chem. Soc.* **1988**, *110*, 1318; b) S. K. Chang, D. Vanengen, E. Fan, A. D. Hamilton, *J. Am. Chem. Soc.* **1991**, *113*, 7640.

[14] K. Motesharei, D. C. Myles, *J. Am. Chem. Soc.* **1998**, *120*, 7328.

[15] J. M. Tour, L. Jones, D. L. Pearson, J. J. S. Lamba, T. P. Burgin, G. M. Whitesides, D. L. Allara, A. N. Parikh, S. Atre, *J. Am. Chem. Soc.* **1995**, *117*, 9529.

[16] H. Valkenier, E. H. Huisman, P. A. van Hal, D. M. de Leeuw, R. C. Chiechi, J. C. Hummelen, *J. Am. Chem. Soc.* **2011**, *133*, 4930.

[17] J. P. Collman, N. K. Devaraj, C. E. D. Chidsey, *Langmuir* **2004**, *20*, 1051.

[18] G. A. Hudalla, W. L. Murphy, *Langmuir* **2009**, *25*, 5737.

[19] G. V. Dubacheva, A. L. Van Der Heyden, P. Dumy, O. Kaftan, R. Auzély-Velty, L. Coche-Guerente, P. Labbé, *Langmuir* **2010**, *26*, 13976.

[20] J. P. Collman, N. K. Devaraj, T. P. A. Eberspacher, C. E. D. Chidsey, *Langmuir* **2006**, *22*, 2457.

[21] A. B. D. Cassie, *Disc. Faraday Soc.* **1948**, *3*, 11.

[22] L. He, J. W. F. Robertson, J. Li, I. Kärcher, S. M. Schiller, W. Knoll, R. Naumann, *Langmuir* **2005**, *21*, 11666.

[23] a) T. Buffeteau, B. Desbat, J. M. Turlet, *Appl. Spectrosc.* **1991**, *45*, 380; b) T. Buffeteau, B. Desbat, D. Blaudez, J. M. Turlet, *Appl. Spectrosc.* **2000**, *54*, 1646; c) M. A. Ramin, G. Le Bourdon, N. Daugey, B. Bennetau, L. Vellutini, T. Buffeteau, *Langmuir* **2011**, *27*, 6076; d) M. A. Ramin, G. Le Bourdon, K. Heuze, M. Degueil, C. Belin, T. Buffeteau, B. Bennetau, L. Vellutini, *Langmuir* **2012**, *28*, 17672.

[24] a) J. G. Radziszewski, J. Michl, *J. Chem. Phys.* **1985**, *82*, 3527; b) A. Bree, R. A. Kydd, *J. Chem. Phys.* **1968**, *48*, 5319; c) G. Socrates in *Infrared Characteristic Group Frequencies*, John Wiley & Sons, New York, **1980**.

[25] R. A. Macphail, H. L. Strauss, R. G. Snyder, C. A. Elliger, *J. Phys. Chem.* **1984**, *88*, 334.

[26] R. G. Snyder, H. L. Strauss, C. A. Elliger, *J. Phys. Chem.* **1982**, *86*, 5145.

[27] a) T. Hasegawa, S. Takeda, A. Kawaguchi, J. Umemura, *Langmuir* **1995**, *11*, 1236; b) C. Naselli, J. F. Rabolt, J. D. Swalen, *J. Chem. Phys.* **1985**, *82*, 2136.

[28] The $N_3C_{12}H_{24}SH/C_{10}H_{21}SH$ molar ratio in the solution used to prepare binary SAMs for these experiments was fixed at 0.1, which corresponds to a surface concentration of azide groups of 20%, according to Figure 4C.

[29] R. Barattin, N. Voyer, *Chem. Commun.* **2008**, 1513.

[30] R. Baron, C. H. Huang, D. M. Bassani, A. Onopriyenko, M. Zayats, I. Willner, *Angew. Chem.* **2005**, *117*, 4078; *Angew. Chem. Int. Ed.* **2005**, *44*, 4010.

[31] a) A. Singh, D. H. Dahanayaka, A. Biswas, L. A. Bumm, R. L. Halterman, *Langmuir* **2010**, *26*, 13221; b) M. I. Béthencourt, L.-O. Srisombat, P. Chinwangso, T. R. Lee, *Langmuir* **2009**, *25*, 1265.

[32] a) H. C. Kolb, M. G. Finn, K. B. Sharpless, *Angew. Chem.* **2001**, *113*, 2056; *Angew. Chem. Int. Ed.* **2001**, *40*, 2004; b) T. Lummerstorfer, H. Hoffmann, *J. Phys. Chem. B* **2004**, *108*, 3963; c) M. Meldal, C. W. Tornøe, *Chem. Rev.* **2008**, *108*, 2952; d) A. González-Campo, S.-H. Hsu, L. Puig, J. Huskens, D. N. Reinhoudt, A. H. Velders, *J. Am. Chem. Soc.* **2010**, *132*, 11434.

[33] a) J. P. Folkers, P. E. Laibinis, G. M. Whitesides, J. Deutch, *J. Phys. Chem.* **1994**, *98*, 563; b) S. J. P. Canete, Z. Zhang, L. Kong, V. L. Schlegel, B. A. Plantz, P. A. Dowben, R. Y. Lai, *Chem. Commun.* **2011**, *47*, 11918.

[34] C. D. Bain, J. Evall, G. M. Whitesides, *J. Am. Chem. Soc.* **1989**, *111*, 7155.

[35] L. Strong, G. M. Whitesides, *Langmuir* **1988**, *4*, 546.

[36] G. McSkimming, J. H. R. Tucker, H. Bouas-Laurent, J. P. Desvergne, S. J. Coles, M. B. Hursthouse, M. E. Light, *Chem. Eur. J.* **2002**, *8*, 3331.

[37] H. Bouas-Laurent, A. Castellan, J.-P. Desvergne, R. Lapouyade, *Chem. Soc. Rev.* **2000**, *29*, 43.

[38] P. Williams in *Scanning Probe Microscopies Beyond Imaging* (Ed.: P. Samorì), Wiley-VCH, Weinheim, **2006**.

[39] For these experiments, the $N_3C_{12}H_{24}SH/C_{10}H_{21}SH$ molar ratio in the solution used to prepare binary SAMs was fixed at 0.01, which corresponds to a surface concentration of azide groups of 2%, according to Figure 4C.

[40] E. Orentas, M. Lista, N.-T. Lin, N. Sakai, S. Matile, *Nat. Chem.* **2012**, *4*, 746.

[41] B. Fabre, D. M. Bassani, C.-K. Liang, S. b. Lhenry, P. Hapiot, *J. Phys. Chem. C* **2013**, *117*, 12725.

Received: April 26, 2013
Revised: June 12, 2013
Published online: August 8, 2013

